Progress In Electromagnetics Research Letters, Vol. 110, 11–19, 2023

Reconfigurable Bandstop Filter with Switchable CLLs for Bandwidth Control

Moheddine Smari[1], Saber Dakhli[1, 2, *], Erwan Fourn[2], and Fethi Choubani[1]

Abstract—In this paper, a compact reconfigurable bandstop filter suitable for multistandard and multiband mobile terminals is reported. The proposed dual bandstop filter consists of a microstrip line coupled to two switchable Capacitively Loaded Loops (CLLs). We achieve the tuning of individual notched frequency bands by using open circuits as switches and incorporated in each CLL element. The performance characteristics in terms of S-parameters and surface currents distribution show that the proposed filter is able to adjust two stopbands independently in a wide tuning range. A corresponding prototype of tunable dual-stopband filter is manufactured, and practical measurements agree well with the simulation results.

1. INTRODUCTION

With the development of new standards and the demand for wireless communications, transceivers that operate over a wide range of frequencies have become crucial. Compact multi-band filters that support multiple standards [1, 2] are key components of such transceivers. In this context, reconfigurability of planar RF filters is a very well-known technique used to tune frequency bandwidths for both reconfigurable microstrip bandpass filters (BPFs) and microstrip bandstop filters (BSFs) designs [3, 4]. In recent researches, several techniques of defected ground structures have demonstrated high performance microstrip reconfigurable bandstop filters [5]. In [6, 7], a compact broadband reconfigurable and frequency tunable structure using split ring rectangular shaped resonators (SRRs) coupled to a coplanar waveguide (CPW) line provided a stopband in the transmission characteristic of the line. A band rejection filter, using CLL elements has been studied in [8]. A switchable BSF presented in [9] is deployed as a decoupling structure for designing a miniaturized reconfigurable multiple input multiple output (MIMO) systems by using the unit cell of SRR. Much more design methods have been investigated in other research works, such as stub-based impedance filters, open-rings, and coupled-line [4]. Electronically, reconfigurable BSFs based on multiple tuning electrical components are generally classified as semiconductor tunable filters (PIN and varactor diodes) [10, 11], RF microelectromechanical systems (MEMS) filters [12, 13], piezoelectric transducers [14], and ferroelectric materials filters [15, 16]. A famous undesired behavior of tunable filters is the variation of bandwidth as the central frequency is changing. This is the result of coupling effect dependency, especially when the active elements of reconfigurability are electronically excited. Several methods have been developed to cope with this problem and to grant and control a constant bandwidth in a given tuning range [17, 18]. In this work, a multi-stopband reconfigurable filter for bandwidth control based on CLLs elements is presented. Through the use of switches employed in each CLL element, we are able to tune individual notched frequency bands.

Received 22 February 2023, Accepted 20 March 2023, Scheduled 28 March 2023
* Corresponding author: Saber Dakhli (saber.dakhli@gmail.com).
[1] Innov'Com Laboratory LR11TIC03, SUPCOM, University of Carthage, Tunisia. [2] University of Rennes, INSA Rennes, IETR, UMR CNRS 6164 Rennes, France.

The manuscript is organized as follows. In Section 2, the proposed reconfigurable RF filter topology, design, and fabrication details are presented. Then, in Section 3, the simulated and experimental performances of the proposed bandstop filter are discussed. Finally, Section 4 summarizes this work and proposes some perspectives.

2. RECONFIGURABLE FILTER'S DESIGN METHODOLOGY

This section describes the methodology followed for the design of the reconfigurable filter. First, we will explain the principle of the chosen reconfigurability and the switching technique. Then we will present the filter's design and fabricated prototype.

2.1. Principle of Reconfigurability

To achieve the reconfigurability of the proposed bandstop filter, we have coupled a rectangular CLL element to a microstrip transmission line. A switch is then incorporated on the CLL in order to control the state of the filter by creating two operating states, "ON" (short-circuit) and "OFF" (open circuit). We note that the CLLs are not restricted to only the rectangular geometry. In this work, the rectangular capacitively loaded loop is chosen because of its relative simplicity of fabrication. In Figs. 1 and 2, we

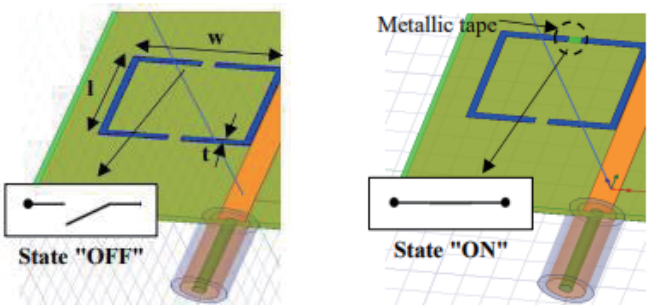

Figure 1. Working principle of the reconfigurable filter with one ideal CLL element: (a) States "OFF" (open circuit) and (b) States "ON" (Short circuit).

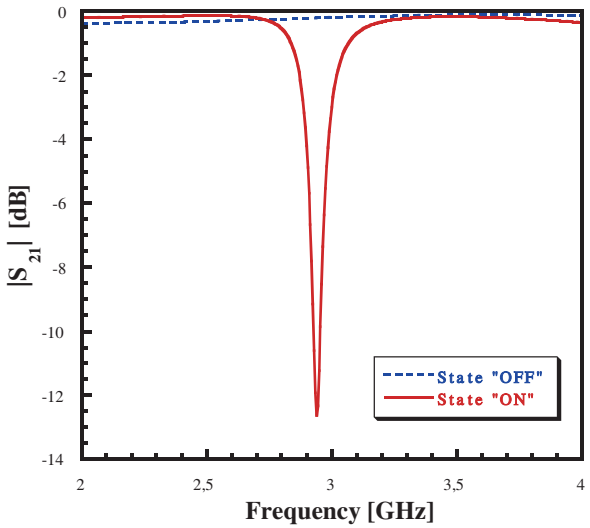

Figure 2. Simulated $|S_{21}|$ parameters of the reconfigurable filter with 1 CLL element related to the states "OFF" and "ON".

explain the working principle of the single CLL in states "ON" and "OFF" and their corresponding S_{21} parameters.

Resonant frequency of the CLL in its "OFF" state is primarily determined by its geometric dimensions. In order to understand the coupling mechanisms and the performance of the filter, the circuit model for a CLL element is explained and developed. In other words, the CLL element is excited by the magnetic fields produced by the transmission line. Through the CLL, it has an extensive net magnetic flux while the effects of an electric-driven gap are insignificant [10]. The magnetically-coupled model based on the results of the magnetic based metamaterial incorporation is shown in Fig. 3. Through the inductor, the source is the flux of the magnetic field, ϕ_H.

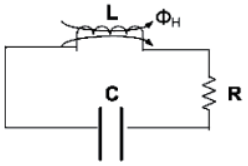

Figure 3. Magnetically-coupled circuit model for the CLL element [10].

Therefore, a CLL element acts like a series RLC circuit fed by a source of current. The resonance frequency of the CLL is given approximately by the following expression [19]:

$$f_{res} = \frac{c}{2L_{CLL}\sqrt{\varepsilon}_{eff}} \tag{1}$$

where L_{CLL} is the total length of the element, ε_{eff} the effective relative dielectric constant, and c the speed of light. Using (1), we can determine the initial total length of the CLL element according to the desired resonance frequency. In order to obtain the final design, numerical simulations can be used to adjust the dimensions of the CLL element.

A multimode filter can be used to reject different bands using the proposed filter. Besides serving as a multi-stop band frequency tunable filter, the proposed structure can also be used to convert its operating frequency into different bands to meet the needs of different wireless applications. In this work, we propose to use two CLL elements to design the reconfigurable filter. More frequency bands can be obtained by adding more CLLs elements to the structure, and the number is not limited to two elements as proposed in this paper.

2.2. Design and Fabrication

In this section, a description on the design and realization of the multi-state filter is discussed. A dual-band RF reconfigurable filter designed to operate at microwave frequencies between 2 and 4 GHz is proposed. It consists of a microstrip line coupled to two different CLLs to obtain two different resonant (notch) frequencies. A switch is incorporated on each CLL in order to achieve the reconfigurability. A deep study of the mapping of the electric field E allows us to determine the adequate gap localization as well as the accommodation of the switches. The proposed structure ($30 \times 30\,\text{mm}^2$) was fabricated on a Rogers Duroid TM5880 substrate with a thickness of 0.8 mm, relative permittivity $\varepsilon_r = 2.2$, relative permeability $\mu_r = 1.0$, and a loss tangent equal to 0.0009. The final reconfigurable filter is shown in Fig. 4. By considering these substrate board material parameters, the width of the 50 Ω-microstrip line is calculated as 2.0 mm. In the filter topology, capacitively loaded loops are coupled with the 50 Ω-microstrip line such that the device can resonate at different frequencies. The structure was simulated and optimized by using the commercially available electromagnetic (EM) simulation software: ANSYS-HFSS v19 high frequency structure simulator.

The proposed filter can be operated as a multimode filter to have different rejected bands. As a multi-stopband frequency tunable filter, the proposed structure can be used to adapt its operating frequencies into different bands serving distinct wireless applications in S-band. We expect that the proposed filter works in four operation modes due to the independent excitation of two CLL elements. The critical dimensions of the microstrip line and all CLL resonators used in the dual-band rejection filter are summarized in Table 1.

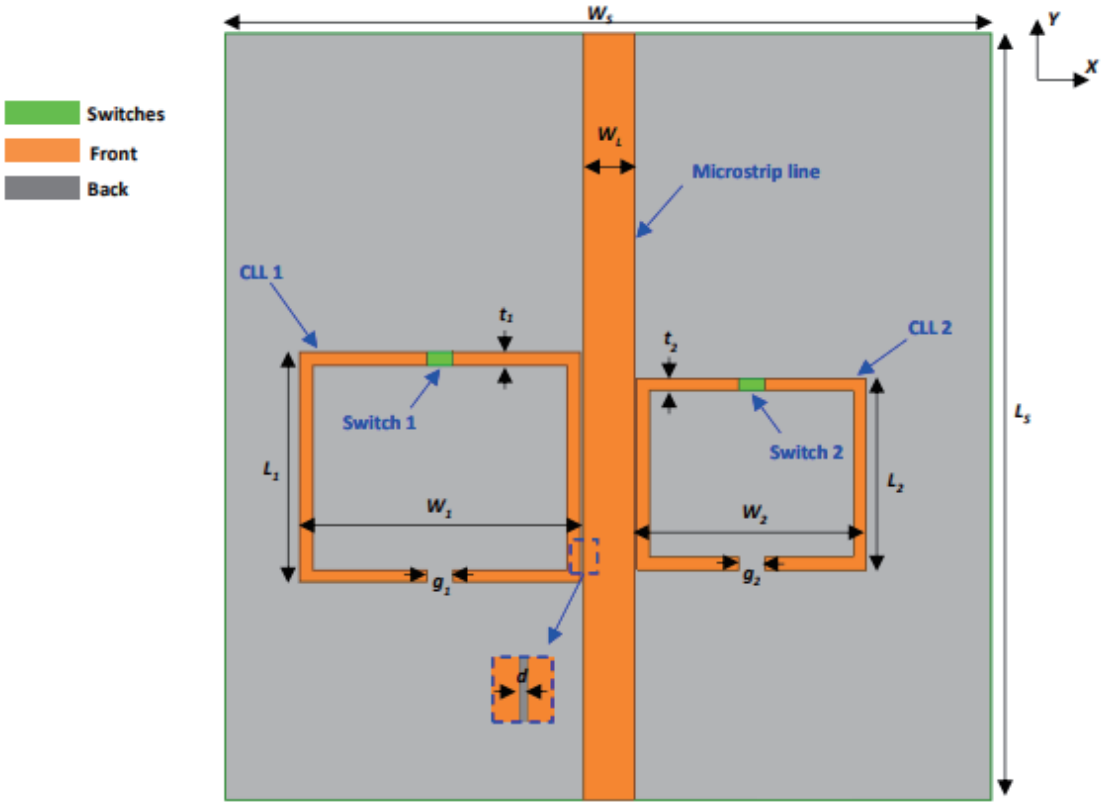

Figure 4. Proposed reconfigurable filter design and dimensions.

Table 1. Design parameters of the reconfigurable filter.

Parameters	L_S	W_S	W_L	L_1	W_1	t_1
Value (mm)	30	30	2	9	11	0.5
Parameters	g_1	L_2	W_2	t_2	g_2	d
Value (mm)	1	7.5	9	0.5	1	0.1

For the experimental validation of our work, a prototype of the planar reconfigurable stop-band filter is manufactured (Fig. 5). The feedline ports are equipped by two 50 Ω SMA coaxial connectors type in both ports. The frequency characterization of the filter is then carried out using the Agilent network analyzer N5230A.

Four modes are obtained for different combinations of switches $S1$ and $S2$ incorporated respectively in the CLL1 and CLL2, as shown in Table 2.

Table 2. Switching modes of the reconfigurable filter.

	S1	**S2**
Mode 1	OFF	OFF
Mode 2	ON	OFF
Mode 3	OFF	ON
Mode 4	ON	ON

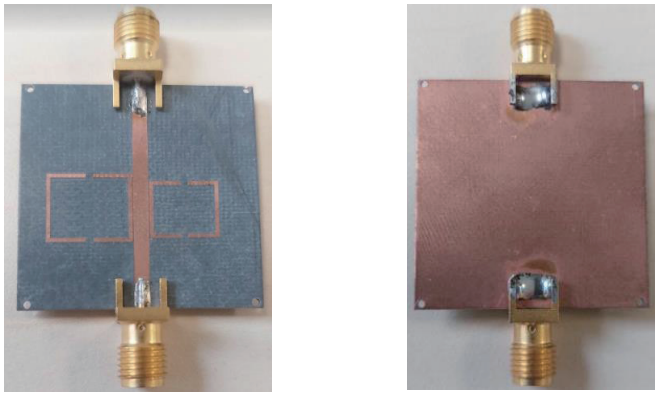

(a) (b)

Figure 5. Fabricated reconfigurable filter: (a) Front view, (b) back view.

To better understand the reconfigurability mechanism, we investigated the surface currents distribution on copper parts in the case of modes 2 and 3 at the resonance frequencies $F_1 = 2.97\,\text{GHz}$ and $F_2 = 3.8\,\text{GHz}$. The simulated surface currents at these two studied rejected frequencies are visible in Fig. 6. As expected, the resonant frequency increases when the lateral dimension of a resonator decreases and inversely. We can also notice that when a CLL resonates, the other does not. It indicates that each of the resonance frequencies could be designed and tuned independently without impacting the other one.

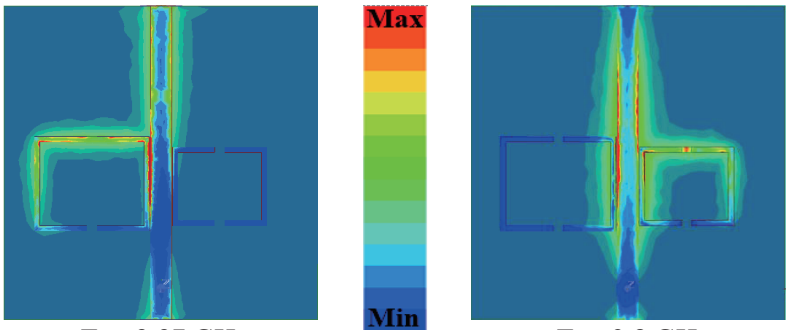

$F_1 = 2.97$ GHz (a) $F_2 = 3.8$ GHz (b)

Figure 6. Simulated surface current distribution corresponding to: (a) mode 2 and (b) mode 3, at the rejected frequencies F_1 and F_2.

3. EXPERIMENTAL RESULTS AND DISCUSSION

In this section, first we present and discuss the simulated and measured results of the proposed reconfigurable bandstop filter in terms of S_{11} and S_{21} related to the four studied modes. Then, a comparative study is presented in order to compare our work with related published results.

3.1. S_{11} and S_{21} Parameters

The transmission and reflection coefficients (S_{21} and S_{11}) of the considered filter have been simulated and measured for all studied modes as shown in Fig. 7. For the experimental case we made a pseudo-reconfiguration of the structure by keeping a real open circuit for the state "OFF" and by filling the gap with metal for the state "ON". In the case of mode 1, when the two resonators are in "OFF" state (Fig. 7(a)), the bandstop filter is without any tuning property. It means that there is no change

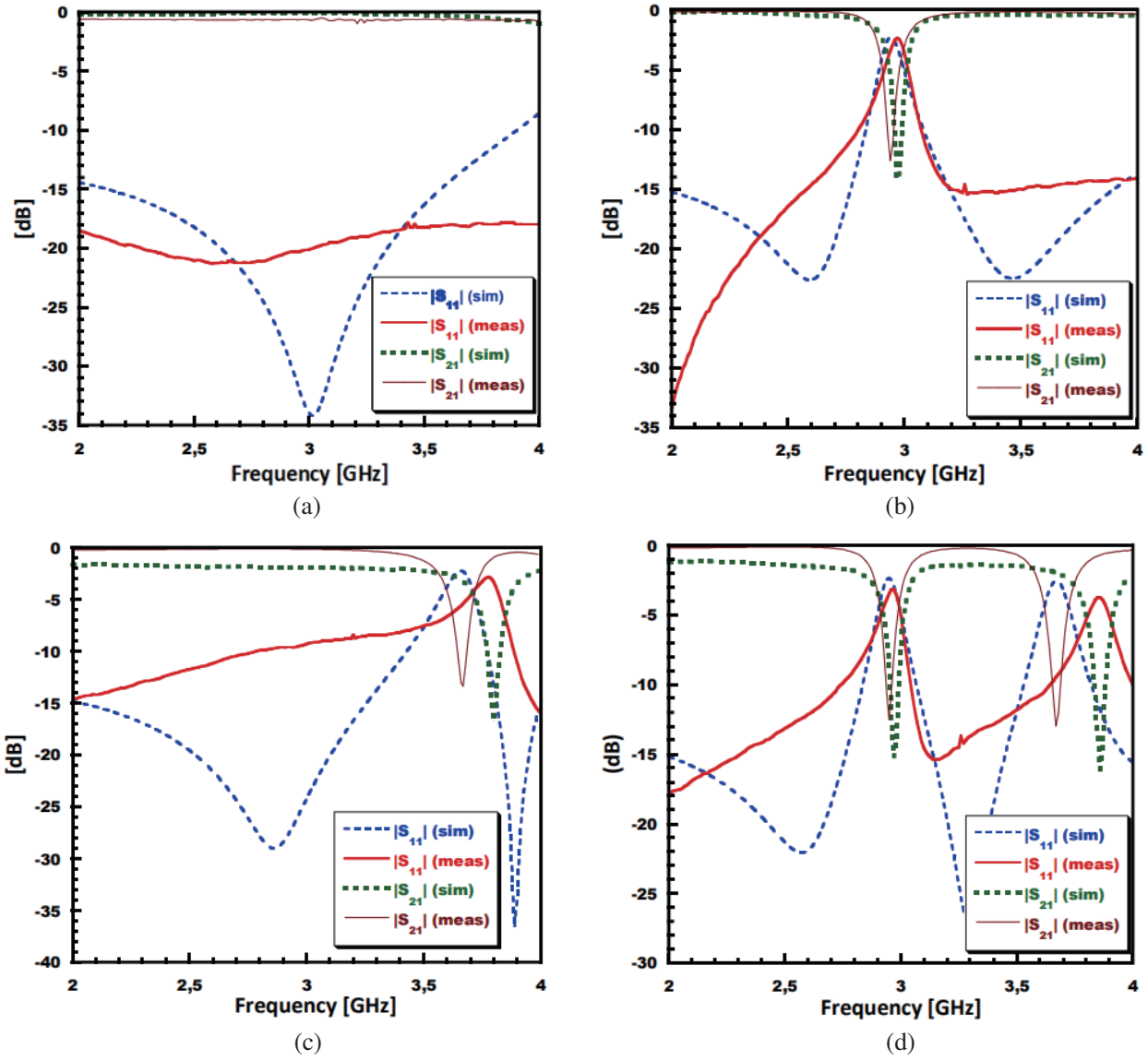

Figure 7. Simulated (sim) and measured (meas) $|S_{11}|$ and $|S_{21}|$ parameters of the reconfigurable filter: (a) mode 1, (b) mode 2, (c) mode 3 and (d) mode 4.

in the magnetic field. For multi-band operations, there are two cases: single-band and dual-band responses. The operating frequencies measured for the single-band rejection behavior (mode 2 and mode 3) are 2.95 GHz and 3.67 GHz respectively (Figs. 7(b) and 7(c)). Dual-band rejection response is obtained when both switches are switched "ON" (mode 4) (Fig. 7(d)). In this case the measured rejected frequencies F_1 and F_2 are located respectively at 2.95 GHz and 3.68 GHz belonging to S-band spectrum. EM simulations and measurements are in good agreement. The slight difference between simulation and measurement results may be explained by the fact that the circuits were fabricated using an LPKF Protolaser U4 for laser engraving. It is possible that a low cost fabrication process can result in some approximation of the line width and a small variation of the dielectric characteristics. The rejected frequencies are summarized in Table 3.

In Table 4, the electrical good performances of the dual bandstop reconfigurable filter corresponding to mode 4 are summarized. Two switches are used to control the center frequencies measured at 2.95 GHz and 3.68 GHz. The bandwidths are equal to 74.5 MHz and 78.2 MHz, respectively, while acceptable insertion losses (between −3.11 and −3.48 dB) and return losses (> 15 dB) are maintained.

Table 3. Simulated (sim) and measured (meas) rejected frequency bands F_1 and F_2 for the four modes.

	$\mathbf{F_1}$ **(GHz)**		$\mathbf{F_2}$ **(GHz)**	
	sim	**meas**	**sim**	**meas**
Mode 1	-	-	-	-
Mode 2	2.97	2.95	-	-
Mode 3	-	-	3.8	3.67
Mode 4	2.97	2.95	3.86	3.68

Table 4. Electrical measured performance of the filter reconfigurable filter corresponding to mode 4.

Band	**Center frequency (GHz)**	**Bandwidth (MHz)**	**Insertion loss (dB)**	**Return loss (dB)**
1	2.95	74.5	−3.11	−15.04
2	3.68	78.2	−3.78	−15.11

3.2. Comparative Study of Related Works

In Table 5, a review of performance comparison between this work and recent reconfigurable bandstop structures available in the literature using different electronic switches is presented. Our proposed prototype has the advantage of simple configuration and tuning giving a wide multifrequency rejection possibility. Besides its compact size, it can be improved further by incorporating real active elements such as PIN diodes to substitute the passive switches used here.

Table 5. Performance comparison with reconfigurable filters available in the state-of-the-art literature.

Ref.	**No of switches**	**Tuning Range (GHz)**	**BW * (MHz)**	**IL ** (dB)**	**Size (mm^3)**	**Lim***/ **Opp****
[20]	2	2.5–3.8	95–115	0.8	$13 \times 8 \times 0.80$	Constant bandwidth
[21]	7	1.7–2.9	40	4	$36 \times 35 \times 0.80$	Number of switches
[22]	4	0.66–0.99	108	0.75	$72 \times 70 \times 1.6$	Low tuning range
[23]	4	2.1–3.9	30–70	1.8	$35 \times 30 \times 0.8$	cost
[This Work]	2	2.97–3.85	74.5–78.2	3	$30 \times 30 \times 0.8$	Non-active switches

*BW: Bandwidth; **IL: Insertion loss; ***Lim: Limitations; *Opp: Opportunities.

4. CONCLUSION

In this paper, a reconfigurable bandstop RF filter has been designed, fabricated, and measured. The proposed structure is composed of a 50 Ω-microstrip line coupled with two capacitively loaded loops (CLLs). Two switches are then integrated, one per CLL element to achieve reconfigurability among four different modes. The notch filtering operation at the rejected frequencies is obtained by activating each CLL switch. The proposed filter has compact size ($30 \times 30\,mm^2$) and is simple to implement. The S-parameters results show a good agreement with the standards specifications in terms of center frequencies and bandwidths, with maintaining acceptable insertion and return losses. The number of rejected bands is not limited to two as presented in this study. Additional frequency bands can be obtained by adding CLLs to the structure in order to meet more requirements of bandwidth control and cognitive wireless applications.

REFERENCES

1. Al-Yasir, Y. I. A., Y. Tu, N. O. Parchin, A. Abdulkhaleq, J. Kosha, A. Ullah, R. Abd-Alhameed, and J. Noras, "New multi-standard dual-wideband and quad-wideband asymmetric step impedance resonator filters with wide stop band restriction," *International J. RF Microwave Computing.*, Vol. 29, 1–17, 2019.
2. Al-Yasir, Y. I. A., Y. Tu, M. S. Bakr, N. O. Parchin, A. S. Asharaa, W. A. Mshwat, R. A. Abd-Alhameed, and J. M. Noras, "Design of multi-standard single/tri/quint-wideband asymmetric stepped-impedance resonator filters with adjustable TZs," *IET Microwave Antennas Propagation*, Vol. 13, 1637–1645, 2019.
3. Tu, Y., Y. I. A. Al-Yasir, N. O. Parchin, A. M. Abdulkhaleq, and R. A. Abd-Alhameed, "A survey on reconfigurable microstrip filter-antenna integration: Recent developments and challenges," *Electronics*, Vol. 9, No. 8, 1249, 2020.
4. Sam, W. Y. and Z. Zakaria, "A review on reconfigurable integrated filter and antenna," *Progress In Electromagnetics Research B*, Vol. 63, 263–273, 2015.
5. Li, Y., S. Luo, and W. Yu, "A compact tunable triple stop-band filter based on different defected microstrip structures," *ACES Journal*, Vol. 33, No. 7, July 2018.
6. Ait Ahmed, B., H. Klaina, O. Aghzout, A. Vazquez Alejos, A. Naghar, and F. Falcone, "Miniaturization, selectivity and rejection bandwidth improvements of a multi-band stopband filter based on circular split ring resonator," *13th European Conference on Antennas and Propagation (EuCAP)*, 2019.
7. Saha, C., J.-Y. Siddiqui, A. P. Freundorfer, L. Shaik, and Y. M. M. Antar, "Active reconfigurable ultra-wideband antenna with complementary frequency notched and narrowband response," *IEEE Access*, Vol. 8, 100802–100809, doi: 10.1109/ACCESS.2020.2997933, 2020.
8. Dakhli, S., M. Smari, J.-M. Floc'h, and F. Choubani, "Microstrip stopband RF filter at microwave frequencies using CLLs elements," *International Conference on Advanced Systems and Emergent Technologies, IC_ASET*, 2020.
9. Islam, H., S. Das, T. Ali, T. Bose, S. Kumari, O. Prakash, and P. Kumar, "Bandstop filter decoupling technique for miniaturized reconfigurable MIMO antenna," *IEEE Access*, Vol. 10, 19060–19071, 2022.
10. Yilong, Z. and D. Yuandan, "Novel dual-band bandpass-to-bandstop filter using shunt PIN switches loaded on the transmission line," *IEEE/MTT-S International Microwave Symposium*, 2020.
11. Guyette, A. C., "Varactor-tuned bandstop filter with tunable centre frequency and bandwidth," *IEEE International Conference on Wireless Information Technology and Systems*, 1–4, Honolulu, 2010.
12. Zhang, N., Z. L. Deng, and F. Sen, "CPW tunable band-stop filter using hybrid resonator and employing RF MEMS capacitors," *IEEE Transactions on Electron Devices*, Vol. 60, No. 8, 2648–2655, 2013.
13. Entesari, K. and G. M. Rebeiz, "A 12–18-GHz three-pole RF MEMS tunable filter," *IEEE Transactions on Microwave Theory and Techniques*, Vol. 53, No. 8, 2566–2571, 2005.
14. Yang, G. M., O. Obi, G. Wen, and N. X. Sun, "Design of tunable bandpass filters with ferrite sandwich materials by using a piezoelectric transducer," *IEEE Transactions on Magnetics*, Vol. 47, No. 10, 3732–3735, 2011.
15. Kato, A., K. Nakatsuhara, and Y. Hayama, "Switching operation in tunable add-drop multiplexer with si-grating waveguides featuring ferroelectric liquid crystal cladding," *Journal of Lightwave Technology*, Vol. 32, No. 22, 4464–4470, 2014.
16. Ghalem, A., F. Ponchel, D. Remiens, and T. Lasri, "A 3.8 GHz tunable filter based on ferroelectric interdigitated capacitors," *IEEE International Symposium on the Applications of Ferroelectric and Workshop on the Piezoresponse Force Microscopy (ISAF/PFM)*, 252–256, Prague, 2013.
17. Xiang, Q. Y., Q. Y. Feng, X. G. Huang, and D. H. Jia, "A 2.285–3.195 GHz electrical tunable bandstop filter with constant absolute bandwidth," *IEEE International Wireless Symposium (IWS)*, 1–4, X'ian, 2014.

18. Arain, S., V. Photos, N. Kashif, Q. Abdul, and S. Nikolaou, "Novel selective feeding scheme integrated with SPDT switches for a reconfigurable bandpass-to-bandstop filter," *IEEE Access*, Vol. 9, 25233–25244, 2021.
19. Lin, C. C., P. Jin, and R. W. Ziolkowski, "Single, dual and tri-band-notched ultrawideband (UWB) antennas using capacitively loaded loop (CLL) resonators" *IEEE Transactions on Antennas and Propagation*, Vol. 60, No. 1, 102–109, January 2012.
20. Al-Yasir, Y., N. O. Parchin, Z.-A. S. A. Rachman, A. Ullah, and R. Abd-Alhameed, "Compact tunable microstrip filter with wide-stopband restriction and wide tuning range for 4G and 5G applications," *Proceedings of the IET's Antennas and Propagation Conference*, 1–6, Birmingham, UK, November 2019.
21. Chen, F., R. Li, and J. Chen, "Tunable dual-band bandpass-to-bandstop filter using p-i-n diodes and varactors," *IEEE Access*, Vol. 6, 46058–46065, 2018.
22. Ebrahimi, A., T. Baum, J. Scott, and K. Ghorbani, "Continuously tunable dual-mode bandstop filter," *IEEE Microwave Wireless Compon. Letter*, Vol. 28, 419–421, 2018.
23. Asci, C., A. Sadeqi, W. Wang, H. R. Nejad, and S. Sonkusale, "Design and implementation of magnetically-tunable quad-band filter utilizing split-ring resonators at microwave frequencies," *Scientific Report*, Vol. 10, No. 1, 1050, 2020.